

P4.4 HIGH-RESOLUTION VERTICAL PROFILES OF TEMPERATURE, WIND SPEED, AND TURBULENCE DURING CASES-99 AND THEIR RELATIONSHIP TO THE TOP OF THE NIGHTTIME BOUNDARY LAYER

Ben Balsley*, Rod Frehlich, Mike Jensen, and Yannick Meillier
University of Colorado, Boulder, Colorado

1. INTRODUCTION

The importance of determining the top of the nighttime stable boundary layer for modeling purposes and for understanding the transport and diffusion of pollutants is well recognized. On the other hand, the difficulty in properly defining this quantity has been discussed in detail by many authors (Nieuwstadt, 1984; Beyrich, 1997; Mahrt, 1998; Seibert, et al., 2000; Zilitinkevitch and Baklanov, 2002; and Mahrt and Vickers, 2003). Techniques used to estimate this height include sodars, lidars, boundary-layer radars, untethered and tethered balloons, instrumented towers, and aircraft. In some instances these measurements estimate the boundary layer top in terms of the zero gradient in the wind profile or the level of maximum potential temperature gradient; other methods estimate the height of the so-called “mixing layer”, or ML. Typically, ML measurements are derived from remote sensing instruments (lidars, sodars, and radars) returns and result from the fact that the scattering processes producing these returns are correlated with turbulent mixing within the boundary layer. Turbulence-related returns are either non-existent or sharply reduced above the top of the stable nighttime boundary layer (NBL). Difficulties in resolving differences in these determinations have been discussed in detail by Beyrich (1997).

During the CASES-99 campaign in east-central Kansas, the CIRES Tethered Lifting System (TLS) of the University of Colorado made some forty high-resolution vertical profiles of temperature, wind speed, and turbulence intensity (Balsley, et al., 2002). Analysis of these nighttime profiles can provide considerable insight into the relationship between the top of the mixing layer height (MH), the height of zero-wind shear, and the height of maximum potential temperature gradient. Here we

examine the MH in terms of high-resolution profiles of the energy dissipation rate, ϵ . The reason for this is that inclusion of comparable (or approximately comparable) values of the temperature structure constant, C_T^2 , would be more confusing and would complicate these presentations.

We show here a number of distinctly different examples of nighttime boundary layer (NBL) structures under a variety of atmospheric conditions. The examples shown below include pertinent parameter profiles of (1) a “traditional stable NBL, (2) a very shallow NBL, and (3) an example of a so-called “upside down” boundary layer, where the turbulence aloft to ~170m altitude is apparently generated entirely by wind shear, since the surface turbulence is prevented from diffusing upward by an very stable low-level inversion and minimal wind shear at ~40m.

2. PROCEDURES

Between two and five turbulence “packages” tethered on a single line suspended from the TLS tether were used during the CASES-99 campaign (Balsley, et. al, 2002; Frehlich, et al., 2002). Each package independently recorded temperature, wind speed, pressure, as well as high-frequency temperature and wind speed data that were converted into turbulence information (i.e., the temperature structure constant, C_T^2 , and the energy dissipation rate, ϵ). In the results shown below, the TLS was operated in a profiling mode, traveling up and down at a rate of approximately 0.4 ms^{-1} . The resulting 1-second-averaged vertical profiles of wind speed and temperature (~ 40 cm vertical resolution) have been approximated by a 10th-order polynomial fit. These fitted profiles have been used to produce profiles of $(dU/dx)^2$, Brunt-Vaisala Frequency (N^2), and Richardson number (Ri). All profiles have been included in the examples for clarity.

3. EXAMPLE OF A “TRADITIONAL” STABLE NBL PROFILE

Figure 1 shows an example of what could be considered to be a “traditional” stable NBL. During

* *Corresponding author address:* Ben Balsley, Cooperative Institute for Research in the Environmental Sciences (CIRES), 216 UCB, University of Colorado, Boulder, CO, 80309, email: Balsley@cires.colorado.edu

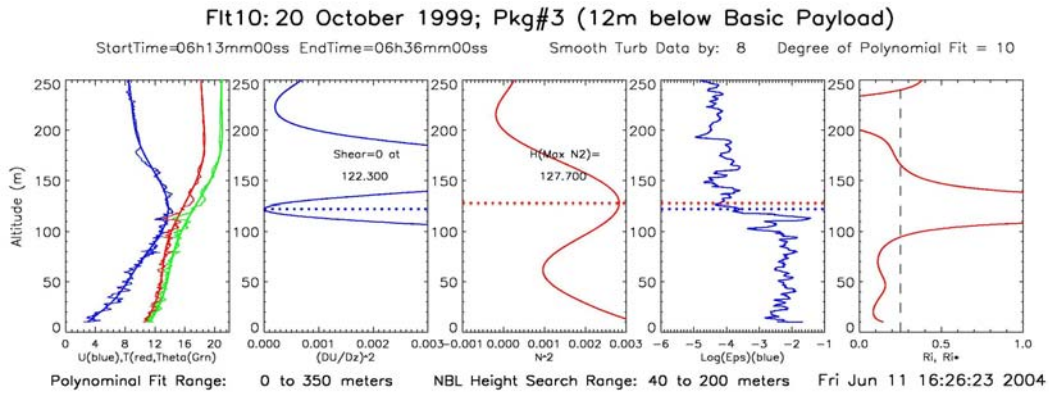


Figure 1. Profiles for 20 October 1999 between 06:13 UT and 06:36 UT. Vertical profiles of 4-second smoothed temperature and wind speed (light, jagged red and blue profiles) in the left-hand panel, along with the darker, smoother profiles obtain using a 10th-order polynomial fitting scheme. These polynomial fitted curved are used to produce the sheared-squared wind speed profile (2nd panel), the Brunt-Vaisala frequency profile (3rd panel), and the Ri profile (right-hand profile). Horizontal dashed lines in the center three panels mark the heights of the minimum $(dU/dz)^2$ and the maximum N^2 within the height range 40m-200m indicated at the bottom of the figure. The 4th panel is a log plot of the turbulence profile epsilon.

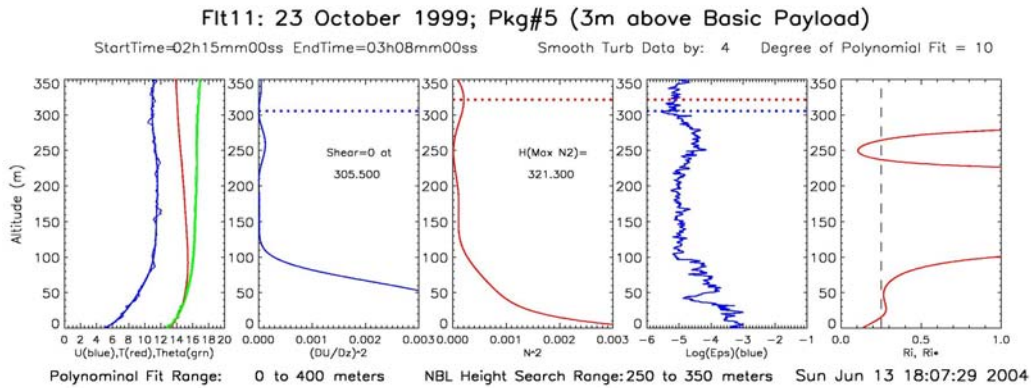


Figure 2. Same as Figure1, except for 23 October 1999 between 02:15 UT and 03:08 UT.

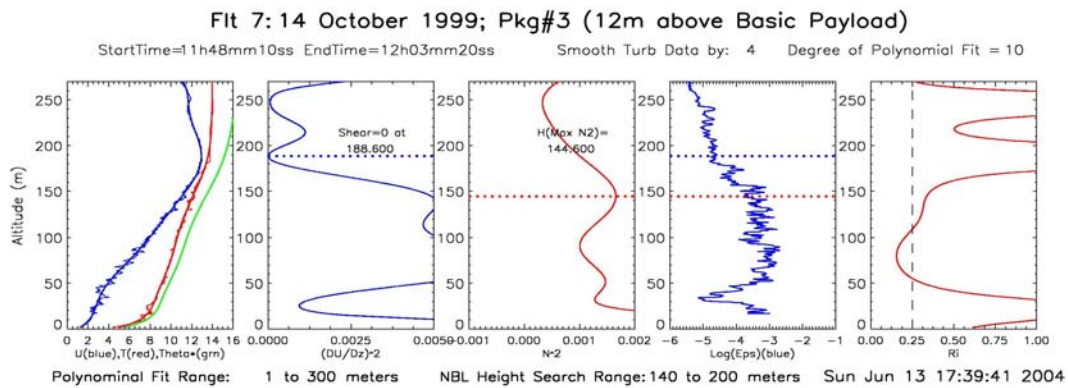


Figure 3. Same as Figure1, except for 14 October 1999 between 11:48 UT and 12:03 UT.

this night (20 October 1999), the lower atmosphere exhibited a monotonically increasing potential temperature profile to at least 250m and a gradually increasing mean wind speed to a height of approximately 129m with the velocity decreasing above that height. The resulting shear-squared profile shows a clear zero minimum at the peak of the wind profile at 122.3m (horizontal dashed blue line in the second panel) while the corresponding N^2 profile has a relative maximum at 127.7m (horizontal dashed red line in the third panel). Both of these heights are shown superimposed on the epsilon (turbulence) profile in the fourth panel.

Note the close correspondence between the two dashed lines and the height at which the turbulence drops sharply by over an order of magnitude. Finally the Ri profile (fifth panel) shows that the entire height range below 100m is unstable ($Ri < 0.25$), with a pronounced (stable) peak in Ri near the ~ 125 m height region delineated by the minimum wind shear, maximum potential temperature gradient, and the sharp decrease in turbulence intensity.

This example can be thought of as a “traditional” stable NBL profile, where a reasonable portion of the turbulence aloft is produced by the near-surface dynamic processes and carried aloft by large-scale turbulence processes and gravity-wave activity. This near-ground-generated turbulence, and that portion of the upper-level turbulence generated aloft by wind shear, is well mixed in the NBL. The upper limit of this mixing is capped by both the zero wind shear at the maximum of the mean wind profile and the region of rapidly changing potential temperature with height (i.e., a maximum in the Brunt-Vaisala frequency, N^2), which combine to produce a large (stable) value of Ri.

Stable nighttime boundary layers of this type have been studied extensively, and appear to be reasonably understood. TLS analysis of this type of NBL during CASES-99 shows a consistent correspondence between the top of the well-mixed layer and the heights of zero wind shear and a maximum in N^2 . It is perhaps significant that the typical height difference between zero wind shear level and the level of N^2 maximum is typically within a few meters. It is also important to point out that the turbulence gradient at the top of the mixed layer can often be in the range of 1 to 2 orders of magnitude *per meter*. While gradients of this

magnitude are surprisingly steep, the TLS results show that they are not uncommon.

4. EXAMPLE OF A SHALLOW NBL

Figure 2 shows an example of a very shallow NBL. During this night (23 October 1999), the lower atmosphere exhibited a moderately increasing potential temperature profile to about 100m with relatively constant values above that height. The wind speed profile exhibited a similar trend, with wind speeds increasing up to about 100m and remaining roughly constant above that height. As indicated in the 2nd and 3rd panels, the deduced profiles of both $(dU/dx)^2$ and N^2 dropped to near zero at about 100m and remained low above that to the maximum observed height on that particular flight. There is no obvious indication of either a pronounced minimum in wind shear squared or a maximum in N^2 , although a slight hint of a minimum in $(dU/dx)^2$ selected by the automated analysis procedure can be discerned at 304m, with a comparable small maximum in N^2 at 321m. Indeed, the only unstable region below 200m appears to lie close to the surface, with the rest of the region being stable.

The strong decrease in the turbulence level with height, and the $\sim 5 \text{ ms}^{-1}$ surface wind suggest strongly that the turbulence is generated near the surface, and is prevented from expanding upward by the stable atmosphere above ~ 50 m. In the absence of a significant minimum in $(dU/dx)^2$ and a maximum in N^2 , it is difficult to assign a height to the top of the ML using these criteria. If we resort to an alternative definition of the top of the mixing layer as the height at which the turbulence level drops by 90% (10 dB), then the top of the ML by that definition is in the vicinity of 100m.

5. EXAMPLE OF AN UPSIDE DOWN NBL

The set of profiles shown in Figure 3 are similar to those shown in Figure 1, with the exception of the steep gradients in both the wind speed and the potential temperature profiles in the first 20m or so. Both a minimum in the shear-squared profile (188m) and a maximum in the N^2 profiles (144m) are apparent in the second and third panels, respectively. A relatively steep drop in turbulence intensity between these two heights is also visible in the third panel. The major difference between the 20 October results in Figure 1 and the current example lies in the steep “bite-out” in the turbulence profile around 30m. The decrease here is greater than two orders of magnitude. Note that

the turbulence level below that height returns to the level of the upper levels.

Examination of the Ri profile (last panel) in Figure 3 shows a marked difference with the Ri profile in Figure 1: While the entire NBL below about 90m in Figure 1 appears to be unstable, there is a pronounced (stable) peak in Ri around 20m in Figure 3, and a region of (possibly) unstable Ri values very close to the surface. The stable region around 20m would prevent the surface-generated turbulence from moving upward to fill the entire NBL. Thus it would appear that the turbulence above 20m derives not from the surface but arises from the unstable regions above 30m-40m and below the top of the mixed layer near 155m, as suggested by the Ri profile.

The concept of these ideas has been embodied in the definition of an “upside down” boundary layer by Mahrt (1998), Ha and Mahrt (2001), Mahrt and Vickers (2002) and discussed further by Banta, et al. (2002) and by Mahrt and Vickers (2003). For an upside down boundary layer the turbulence is generated by shear in the low-level nocturnal jet.

6. CONCLUSIONS

The above results should be considered as only a preliminary study of the relationship between high-resolution vertical profiles of temperature, wind speed, and turbulence and the top of the nighttime boundary layer. The results are representative, however, of some forty separate vertical profiles obtained during CASES-99 under a wide range of conditions.

In the majority of these profiles there was a good-to-excellent correspondence between the mixing height and the height of a zero value of $(dU/dx)^2$ and a relative maximum of the Brunt-Vaisala Frequency (N^2), where these values indicated a maximum in the wind profile and the steepest portion of the potential temperature profile, respectively. MH levels during CASES-99 ranged between a low of 15m and a high of 200m.

Our analyses also show clear examples when there is an absence of a distinct peak in the wind profile (zero shear) and a corresponding absence of a measurable maximum in the N^2 profile. In these instances, the mixing heights do not appear to be correlated with inflections in the mean wind speed and potential temperature profiles, but rather reflect the height where the Ri number becomes strongly positive.

It appears that the TLS technique can be a promising tool for studying the relationship between nighttime boundary layer turbulence processes and the associated wind and temperature profiles. The fundamental advantage of TLS *in situ* sampling lies with its high-resolution capability (sample rates of >200 Hz combined with the slow track of the sensors through the atmosphere). TLS data on wind speed/direction, temperature, as well on ϵ and C_T^2 should provide critical information for calibrating remote sensing instruments such as lidars, FMCW radars and boundary layer radars.

REFERENCES

- Balsley, B. B., R. G. Frehlich, M. L. Jensen, Y. Meillier, and A. Muschinski, 2003: Extreme Gradients in the Nocturnal Boundary Layer: Structure, Evolution, and Potential Causes, *Jour. Atm. Sci.*, **15**, 2496-2508, 2003.
- Banta, R., R. K. Newsom, J. K. Lundquist, Y. L. Pichugina, R. L. Coulter, and L. Mahrt, 2002: Nocturnal low-level jet characteristics over Kansas during CASES-99, *Boundary-Layer Meteorology*, **105**, 221-252.
- Banta, R., Y. L. Pichugina, and R. K. Newsom, 2003: Relationship between low-level jet properties and turbulent kinetic energy in the nocturnal stable boundary layer, *Notes and Correspondence, J. Atmos. Sci.*, **60**, 2549-2555.
- Beyrich, F., 1997: Mixing height estimation from sodar data-A critical discussion, *Atmospheric Environment*, **31**, 3941-3953.
- Frehlich, R. G. Y. Meillier, M. L. Jensen, B. B. Balsley, 2003: Turbulence Measurements with the CIRES TLS (Tethered Lifting System) during CASES99, *Jour. Atm. Sci.*, 2487-2495.
- Ha, K. J. and L. Mahrt, 2001: Simple inclusion of z-less turbulence within and above the modeled nocturnal boundary layer, *Monthly Weather Rev.*, **129**, 2136-2143.
- Joffre, S. M., M. Kangas, M. Heikenheimo, and S. A. Kitaigorodskii, 2001: Variability of the stable and unstable atmospheric boundary height and its scales over a boreal forest, *Boundary-Layer Meteorology*, **99**, 429-450.

- Mahrt, L., 1998: Stratified atmospheric boundary layers, *Boundary-Layer Meteorology*, **90**, 375-396.
- Mahrt, L. and D. Vickers, 2002: Contrasting Vertical Structures of nocturnal boundary layers, *Boundary-Layer Meteorology*, **105**, 351-363.
- Mahrt, L. and D. Vickers, 2003: Formulation of turbulent fluxes in the stable boundary layer, *J. Atmos. Sci.*, **60**, 2538-2548.
- Neiustadt, F. T. P., 1984: Some aspects of the turbulent stable boundary layer, *Boundary-Layer Meteorology*, **30**, 31-55.
- Seibert, P., FR. Beyrich, S. E. Gryning, S. Joffre, A. Rasmussen, and P. Tercier, 2000: Review and intercomparison of operational methods for the determination of the mixing height, *Atmospheric Environment*, **34**, 1001-1027.
- Zilintinkevich, S. and A. Baklanov ,2001: Calculation of the height of the stable boundary layer in practical applications: *Boundary-Layer Meteorology*, **105**, 389-409.